Induced Transparency by Intersubband Plasmon Coupling in a Quantum Well

Jianzhong Li* and C. Z. Ning†
Center for Nanotechnology, NASA Ames Research Center, Mail Stop N229-1, Moffett Field, California 94035, USA
(Received 1 March 2004; published 19 August 2004)

We study coupling of two intersubband plasmons associated with dipole-allowed cascading transitions in a quantum well. We show that the coupling can lead to the disappearance of the lower-energy resonance accompanied by an anticrossing behavior. Such coupling induced anomalies are of collective and resonant nature and provide the first example of Coulomb interaction induced transparency. Our numerical results from a microscopic theory are confirmed by an analytical model.

DOI: 10.1103/PhysRevLett.93.087402 PACS numbers: 78.67.De, 73.21.Fg, 78.20.Bh, 78.30.Fs

One of the most fundamental features of an interacting system is the formation of various collective excitations (CXs) [1,2]. Their mutual couplings lead to the creation of new CXs and can renormalize the properties of a many-body system in a nontrivial manner. CXs in the context of intersubband transitions, such as intersubband plasmon (ISP) and intersubband exciton (or repellon) [3–5], are especially interesting, since the transition energies can be comparable to the energies of these CXs. Besides their importance in fundamental physics, dramatical spectral changes resulting from these CXs, and their couplings in quantum wells (QWs) have important technological consequences, since intersubband resonances (ISBRs) are the physical basis for light generation and detection in the long wavelength range from the mid to far infrared.

Various CXs and coupling mechanisms involving ISBRs have been studied. These include an ISP coupled with an intrasubband plasmon [6], a longitudinal optical (LO) phonon [7,8], a surface plasmon [9], and a cavity mode (leading to an intersubband polariton) [10]. One of the interesting cases that has so far eluded theoretical attention is a QW with at least three subbands [11], where the two lowest subbands are populated such that cascading transitions from both subbands are possible. Since each ISBR is a polarizable CX, a natural question arises: What happens when two ISBRs are coupled? In this Letter, we report, to the best of our knowledge, the first case of spectral transparency induced by an out-of-phase many-body coupling between two intersubband CXs.

We consider a symmetric QW with three subbands (labeled as 1, 2, and 3 from low to high energy, respectively) with cascading transitions from 1 to 2 ($1 \to 2$) and from 2 to 3 ($2 \to 3$). Direct transition from 1 to 3 is dipole forbidden. We focus on the situation where the depolarization effect dominates, or where the ISP is the dominant CX. From studies of ISBRs with two subbands [4,5], this happens when the QW thickness (W) is large or electron density is high. For semiconductors with weak nonparabolicity such as GaAs, ISPs are almost always the dominant CXs. We study in detail the coupling of ISPs associated with $1 \to 2$ and $2 \to 3$ transitions and its consequences on the absorption spectrum. Typically, linear coupling between two CXs or oscillators leads to the usual anticrossing phenomenon. We show that, in addition to this standard behavior, the linear ISP coupling leads to the disappearance of the lower-energy resonance at anticrossing. Such many-body induced transparency (diminished absorption) occurs due to destructive superposition of the ISP components at anticrossing, as both the existence and coupling of the ISPs have sole origin in Coulomb interaction. We suggest that custom-designed QWs with specific electron populations could lead to the observation of the induced transparency.

Our theoretical approach follows the semiconductor Bloch equations developed for interband transitions [2,12], which have recently been applied to the two-subband case [4,5,13–15]. The extension to multisubband cases is straightforward. Our starting point [16] is a Hamiltonian including quantum confinement, Coulomb interaction among charged carriers (both electrons and donors), and light-electron interaction. Derivation of the equations of motion from the Hamiltonian results in a set of intersubband semiconductor Bloch equations. The equation for intersubband polarization $p_{\boldsymbol{k}}^{mn}$ between subband m and n is given as follows (in the Fourier domain):

$$[(\hbar\omega + i\gamma_{mn}) - (\varepsilon_{nk} - \varepsilon_{mk})]p_{\boldsymbol{k}}^{mn} = (-\boldsymbol{d}_{\boldsymbol{k}}^{mn} \cdot \boldsymbol{E}_0 + \varepsilon_{\boldsymbol{k}}^{mn})(f_{mk} - f_{nk}) - \sum_{j,\boldsymbol{q}}^{l\neq m, l\neq n} f_{jk+q}(V_{\boldsymbol{q}}^{njlj} p_{\boldsymbol{k}}^{ml} - V_{\boldsymbol{q}}^{ljmj} p_{\boldsymbol{k}}^{ln}), \tag{1}$$

where $\boldsymbol{k}, \boldsymbol{q}$ are in-plane wave vectors, ω is the angular frequency of the incident light of amplitude $\boldsymbol{E}_0$, $\gamma_{mn}/\hbar$ is the dephasing rate [17], $\boldsymbol{d}_{\boldsymbol{k}}^{mn}$ is the dipole matrix element (assumed $\boldsymbol{k}$ independent in our numerical solution, or $\boldsymbol{d}_{\boldsymbol{k}}^{mn} = \boldsymbol{d}_{mn}$), and f_{mk} is the Fermi-Dirac distribution function. $V_{\boldsymbol{q}}^{ljmn}$'s are Coulomb matrix elements (superscripts indicating subband indices; see [13]). The single-particle energy (ε_{mk}) with self-energy correction and the "local field" correction ($\varepsilon_{\boldsymbol{k}}^{mn}$) are, respectively, given by

$$\varepsilon_{mk} = E^{(0)}_{mk} - \sum_{l,q} V^{mlml}_{q} f_{lk+q}, \tag{2}$$

$$\varepsilon^{mn}_{k} = -\sum_{j\neq l,q} V^{njml}_{q} p^{jl}_{k+q} + \sum_{j\neq l,q} V^{njlm}_{0} p^{jl}_{q}. \tag{3}$$

$E^{(0)}_{mk}$'s can be obtained from a self-consistent band structure calculation including quantum confinement effect and the Hartree potential. The local field correction comprises a Fock term (V^{njml}_{q}) that yields the intersubband exciton (or repellon [4]) and a Hartree term (V^{njlm}_{0}) that introduces ISPs [4,5]. When deriving the above equations, linearization in the polarization p^{mn}_{k} has been made. As can be seen from Eqs. (1)–(3), ISP coupling arises because each ISP (p^{jl}_{k}) modifies the local field experienced by another one (p^{mn}_{k}). Therefore such coupling is of resonant and collective nature. Note that p^{mn}_{k}'s are completely decoupled in the absence of Coulomb interaction ($\varepsilon^{mn}_{k} = 0$) in the linear regime. Thus the situation here provides a unique example where not only the existence of individual CXs and their coupling have the same origin in Coulomb interaction, but, most importantly, the linear and resonant coupling could also lead to the destruction of a particular CX. It is the focus of this Letter to study the effects of such a coupling on the ISBRs.

ISBRs can be described by absorbance defined as $\omega W \mathrm{Im}[\chi(\omega)]/nc$, where $\chi(\omega)$ is the optical susceptibility, n is the background refractive index, and c is the speed of light *in vacuo*. $\chi(\omega) \equiv P/\varepsilon_0 E_0$ and the material polarization $P = 2S/[(2\pi)^2 \mathcal{V}]\sum_{mn}\int d\boldsymbol{k} d^{mn*}_{k} p^{mn}_{k} = d_{12}P_{12} + d_{23}P_{23}$. ε_0 is the electric constant and $\mathcal{V} = WS$, where S is a normalization area. We numerically solved Eq. (1) for p^{mn}_{k} by a matrix inversion method. The parameter values are given in Fig. 1. V^{njml}_{q}'s and D_{njml}'s (depolarization factors, $\equiv V^{njml}_{0}$) were evaluated with the quantum box model. Conduction band nonparabolicity was represented by unequal masses (m_i, $i = 1, 2, 3$) for the three parabolic subbands. We further assumed $\gamma_{mn} = 1$ meV. It was checked that the rotating wave approximation is applicable and that the last term (direct interference Coulomb interactions) on the right-hand side of Eq. (1) plays a negligible role.

Figure 1 shows a series of absorbance spectra as band edge separation of the two upper subbands, E_{32}, is varied, while the band edge separation of the two lower subbands, E_{21}, is fixed to 50 meV, which is the value for a 15 nm square GaAs QW with infinite barriers. The density is so large that ISPs dominate, whereas repellons are greatly weakened by screening and thus are negligible [5]. There are two striking features in the spectra. First, we see an anticrossing behavior. Second, but most important, the lower-energy resonance vanishes at the anticrossing point. To understand this phenomenon of vanished absorption (or transparency), we show in Fig. 2 contributions from individual polarization components to absorbance. From the inset, we see that ISPs are the dominant CXs, as the solid and the long dashed curves are almost identical.

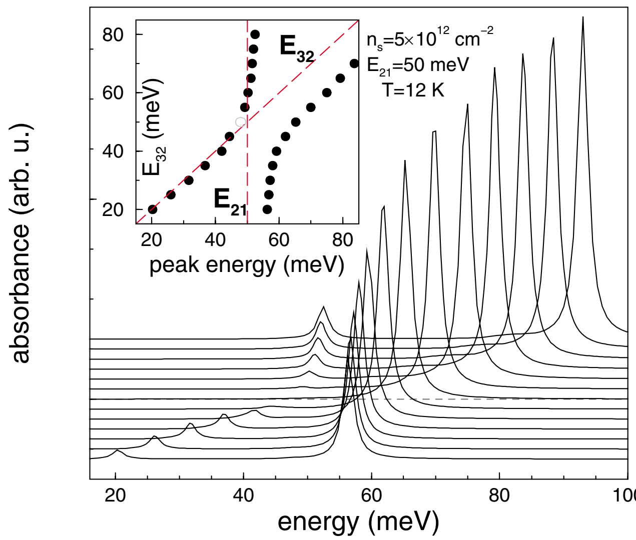

FIG. 1 (color online). Intersubband spectra of a GaAs quantum well. Different curves, offset for clarity, correspond to E_{32} (upper subband separation at $\boldsymbol{k} = 0$) tuned from 20 to 80 meV with a 5 meV interval. Inset shows peak energy as a function of E_{32}. The open circle indicates where an induced transparency occurs at the lower-energy resonance. Parameter values used: $m_1 = 0.068m_e$, $m_2 = 0.073m_e$, $m_3 = 0.080m_e$; $d_{12} = -33.5$ e Å and $d_{23} = -37.6$ e Å.

This justifies our ensuing analysis where we will explain the results solely in terms of ISPs. The lower-energy resonance practically vanishes, leaving a small bump on the full and ISP curves (near the position of the single-particle resonance). The bump remains due to the finite

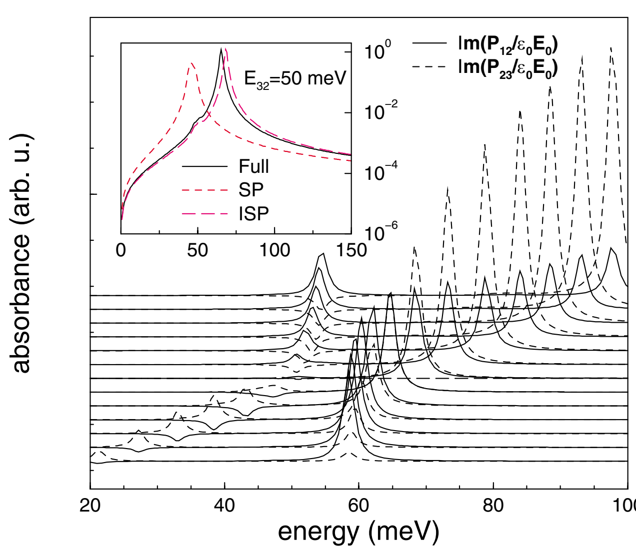

FIG. 2 (color online). Absorbance associated with individual polarization components P_{12} and P_{23}. The inset shows absorbance in linear-log scale: single-particle (SP) spectrum (dashed curve) consisting of two nearly degenerate transitions, Hartree-Fock (Full) result (solid curve) showing a narrowed and blue shifted single-resonance spectrum, and the Hartree (ISP) spectrum (long dashed curve).

dephasing rate. The separation between the bump and the main peak to its right is the anticrossing splitting, estimated to be about 18 meV. The single-particle spectrum consists of two degenerate resonances: $1 \rightarrow 2$ and $2 \rightarrow 3$. Now we examine the figure itself and explain the reason for choosing a symmetric QW and a three-subband model. Symmetry dictates that only two cascading transitions ($1 \rightarrow 2$ and $2 \rightarrow 3$) are dipole allowed. The corresponding depolarization factors are D_{1122} and D_{2233}. Furthermore, only one depolarization factor (D_{1232}) survives that couples the two otherwise independent ISPs. This coupling leads to the anticrossing behavior and transparency in lower-energy resonance. Without such coupling, the three-subband system is reduced to two independent two-subband systems. The two resonances will simply cross each other as we sweep the upper subband separation (see inset of Fig. 1, dashed curves). Because of the coupling, we see that both the individual components (Fig. 2) and the total absorbance (Fig. 1) show a reduction of oscillator strength in the lower-energy resonance and enhancement in the upper-energy resonance. Note that the higher energy ISP component always makes an out-of-phase contribution to the lower-energy resonance. For example, the P_{12} contribution to $2 \rightarrow 3$ is negative before the anticrossing, whereas the P_{23} component contributes to $1 \rightarrow 2$ negatively after the anticrossing. While contributions from individual components are decreasing as we approach the anticrossing point, the out-of-phase superposition further reduces the total oscillator strength of the lower-energy resonance [also cf. Eqs. (4) and (5)]. At the anticrossing point, both the decreasing individual components and their out-of-phase superposition lead to the disappearance of absorption at the lower-energy resonance, or a transparency induced purely by Coulomb interaction. We believe that this is the only known example where the interaction causes a full out-of-phase coupling of the two collective excitations and the consequent transparency.

To gain further insights and to corroborate the simulation results presented above, we consider a limiting case where Eq. (1) can be solved analytically. To this end, we assume that the Fock terms in the self-energy and local field correction can be ignored, and so can the last term in Eq. (1). Our numerical results (see inset of Fig. 2) show that these are good approximations for the GaAs QWs. This is not surprising because of an exact cancellation of all Fock terms in the case of a parabolic bulk band [14,15]. To be consistent, we assume equal masses for all three subbands. Under these approximations, Eq. (1) is integrated over $\boldsymbol{k}$ and simplified as follows:

$$(\hbar\omega - E_{21} + i\gamma_{12})P_{12} = (-d_{12}E_0 + D_{1122}P_{12} + D_{1232}P_{23})n_{12}, \tag{4}$$

$$(\hbar\omega - E_{32} + i\gamma_{23})P_{23} = (-d_{23}E_0 + D_{2233}P_{23} + D_{1232}P_{12})n_{23}, \tag{5}$$

where $n_{jl} = n_j - n_l = \sum_k (f_{jk} - f_{lk})/S$. The equation for P_{13} is decoupled from these two equations and will not be further discussed. These two equations are illuminating. They would be decoupled without the depolarization term, D_{1232}. There are two types of depolarization terms: D_{iijj} ($i \neq j$) and D_{1232}. The former can be collected into the left-hand side of Eqs. (4) and (5) by defining a new transition energy, $\tilde{E}_{ij} = E_{ij} + D_{jjii}n_{ji}$. This is the well-known result of the depolarization shift when both subbands are populated. The latter, D_{1232}, introduces coupling between the two polarizations P_{12} and P_{23} and thus can be termed as the mutual depolarization effect. Obviously, this is a pure collective coupling. Accordingly, we call terms D_{1122} and D_{2233} self-depolarization terms. Whereas the self-depolarization terms lead to the formation of ISPs, the mutual depolarization term introduces coupling between such ISPs.

A closed form solution of the total polarization $P = d_{12}P_{12} + d_{23}P_{23}$ can be obtained as follows:

$$P = -\left[\frac{(\delta E_{32} + i\gamma_{23})d_{12}^2 n_{12} + (\delta E_{21} + i\gamma_{12})d_{23}^2 n_{23} + 2D_{1232}n_{12}d_{12}n_{23}d_{23}}{(\delta E_{21} + i\gamma_{12})(\delta E_{32} + i\gamma_{23}) - D_{1232}^2 n_{12}n_{23}}\right]E_0, \tag{6}$$

where $\delta E_{ij} = \hbar\omega - \tilde{E}_{ij}$. Under resonance condition, i.e., $d/d\omega[\mathrm{Im}(P/E_0)] = 0$, the resonance amplitude $[\mathrm{Im}(P/E_0)]$ at $\delta E_{21} = 0$ is proportional to

$$\frac{\gamma_{12}n_{12}d_{12}^2}{\gamma_{12}^2 - D_{1232}^2 n_{12}n_{23}} + \frac{(\gamma_{12} + \gamma_{23})n_{12}d_{12}n_{23}d_{23}D_{1232}}{\delta E_{32}(\gamma_{12}^2 - D_{1232}^2 n_{12}n_{23})}, \tag{7}$$

which is rather illuminating: the contribution due to the ISP coupling (second term) is proportional to $1/\delta E_{32}$ and diverges at the anticrossing point. Therefore, we expect a large effect *and* a change of sign at anticrossing when E_{32} is tuned, from positive below resonance to negative above resonance, as evidenced in Fig. 2. The resonance frequencies ($\omega_\pm$) can be approximated by the poles of Eq. (6) with $\gamma_{12} = \gamma_{23} = 0$. They show an anticrossing behavior, and the minimum separation is given by

$$\hbar(\omega_+ - \omega_-)_{\min} = 2D_{1232}\sqrt{n_{12}n_{23}}, \tag{8}$$

when $\tilde{E}_{21} = \tilde{E}_{32}$. To explain the transparency, we calculate $\mathrm{Im}(P/E_0)$ with $\gamma_{12} = \gamma_{23} = \gamma$ at anticrossing ($\tilde{E}_{21} = \tilde{E}_{32}$). The numerator is given by

$$2D_{1232}^2 n_{12}n_{23}[d_{12}\sqrt{n_{12}} \pm d_{23}\sqrt{n_{23}}]^2 + \gamma^2(n_{12}d_{12}^2 + n_{23}d_{23}^2), \tag{9}$$

with the denominator being $\gamma(4D_{1232}^2 n_{12}n_{23} + \gamma^2)$. At high density, the ratio $2D_{1232}^2 n_{12}n_{23}/\gamma^2$ is of the order of 100 so that the lower-energy resonance [with minus sign in the first term in Eq. (9)] is suppressed by the same order of magnitude (thus transparency; see inset of Fig. 2) at anticrossing when $d_{12}\sqrt{n_{12}} = d_{23}\sqrt{n_{23}}$. In sum, the analytical conditions for observing the induced transparency are as follows: (i) the two renormalized frequencies are degenerate ($\tilde{E}_{21} = \tilde{E}_{32}$); and (ii) the oscillator strengths ($\propto d_{ij}^2 n_{ij} \tilde{E}_{ji}$) match exactly ($d_{12}\sqrt{n_{12}} = d_{23}\sqrt{n_{23}}$). The second condition can be used to estimate the required doping density (n_s), which is given by $n_s = [1 + 2(d_{12}/d_{23})^2]\rho_{2D}E_{21}$ at zero temperature, where $\rho_{2D} = m^*/\pi\hbar^2$ is the 2D density of states. For the GaAs QW examined in this Letter, we have $n_s \approx 3.8 \times 10^{12}$ cm^{-2}, in reasonable agreement with the electron density used in the simulation.

It is known that conduction band nonparabolicity weakens ISPs and enhances intersubband excitons [5]. We therefore studied the coupling of ISPs in InAs, a representative material with strong nonparabolicity. We found indeed that both the individual ISPs and their coupling are very much weakened. The feature of a disappearing resonance is no longer clearly visible.

We comment briefly on possible experimental observation of the spectral anomalies reported in this Letter. A possible candidate is to use a symmetric step quantum well where the lowest two subbands are more or less determined by the center portion of the well, while the outer layer thickness can be varied to adjust the upper subband separation. Other symmetric structures with continuous grading are also possible. In addition, it is important to have large enough resonance energies in order to differentiate the induced transparency from other mechanisms, such as ISP-LO phonon coupling [8]. Furthermore, the QW thickness is not a critical parameter, much less critical than the coupling depolarization factor D_{1232}, which has to be as large as D_{1122} and D_{2233}. A one-third reduction in D_{1232} would practically diminish the coupling effect, as our simulations indicated (not shown). Finally, the QW needs to be properly doped such that the two ISP components have similar oscillator strengths for the induced transparency to occur.

In conclusion, we have studied the coupling of intersubband plasmons associated with two cascading transitions among three subbands in a quantum well, where both the existence of the individual plasmons and their coupling are due to the Hartree interaction. We show that the coupling renders an absorption peak transparent, while the resonances exhibit an otherwise typical anticrossing behavior. We believe that this is the first example of transparency induced by pure many-body Coulomb interaction. Such a phenomenon not only enriches our understanding of many-body physics in intersubband transitions, but it could also open a new way to achieve transparency in intersubband transitions, a technologically important field of research.

The authors are with UARC (the University Affiliated Research Center) at NASA Ames Research Center, managed by UC, Santa Cruz. This work was supported by AFOSR and a joint NASA-NCI program.

*Electronic address: jnli@mail.arc.nasa.gov
†Electronic address: cning@mail.arc.nasa.gov
http://www.nas.nasa.gov/~cning

[1] H. Haken, *Quantum Field Theory of Solids, An Introduction* (North-Holland, New York, 1976); G. D. Mahan, *Many-Particle Physics* (Plenum Press, New York, 1981).
[2] H. Haug and S.W. Koch, *Theory of the Electrical and Optical Properties of Semiconductors* (World Scientific, Singapore, 1994).
[3] S. J. Allen, D. C. Tsui, and B. Vinter, Solid State Commun. **20**, 425 (1976); D. A. Dahl and L. J. Sham, Phys. Rev. B **77**, 651 (1977); T. Ando, A. B. Fowler, and F. Stern, Rev. Mod. Phys. **54**, 437 (1982); J. C. Ryan, Phys. Rev. B **43**, 12 406 (1991); R. J. Warburton *et al.*, Phys. Rev. Lett. **80**, 2185 (1998).
[4] D. E. Nikonov *et al.*, Phys. Rev. Lett. **79**, 4633 (1997).
[5] J. Li and C. Z. Ning, Phys. Rev. Lett. **91**, 097401 (2003).
[6] S. Das Sarma, Phys. Rev. B **29**, 2334 (1984); S. Oelting, D. Heitmann, and J. P. Kotthaus, Phys. Rev. Lett. **56**, 1846 (1986); L. Wendler and V. G. Grigoryan, Solid State Commun. **71**, 527 (1989).
[7] L. Wendler, R. Haupt, and V. G. Grigoryan, Physica (Amsterdam) **167B**, 113 (1990); D. Richards, J. Wagner, and J. Schmitz, Solid State Commun. **100**, 7 (1996).
[8] H. C. Liu *et al.*, Phys. Rev. Lett. **90**, 077402 (2003).
[9] P. Hawrylak, J.-W. Wu, and J. J. Quinn, Phys. Rev. B **32**, 5169 (1985).
[10] D. Dini *et al.*, Phys. Rev. Lett. **90**, 116401 (2003).
[11] S. Tsujino *et al.* (unpublished); K. T. Lai *et al.*, J. Appl. Phys. **93**, 6065 (2003).
[12] W.W. Chow and S.W. Koch, *Semiconductor-Laser Fundamentals* (Springer-Verlag, Berlin, 1999).
[13] T. Kuhn, in *Theory of Transport Properties of Semiconductor Nanostructures*, edited by E. Schöll (Chapman & Hall, London, 1998).
[14] I. Waldmüller *et al.*, Phys. Rev. B **69**, 205307 (2004).
[15] J. Li and C. Z. Ning, Phys. Rev. B (to be published).
[16] C. Z. Ning and J. Li, Proc. SPIE Int. Soc. Opt. Eng. **5352**, 284 (2004).
[17] As we showed in [15], detailed second order scattering terms introduce quantitative, albeit large, changes to the linewidth. But the dephasing rate approximation would not introduce qualitative changes to the intersubband absorption spectrum for GaAs. Therefore, the dephasing rate approximation is adequate and avoids unnecessary complications. Furthermore, the same rate is assumed for all transitions.